Journal of Engineering Science, Vol. 15, 11–21, 2019

Transformation of Magnetite (Fe_3O_4) and Maghemite (γ–Fe_2O_3) to a–Fe_2O_3 from Magnetic Phase of Glagah Iron Sand

Sayekti Wahyuningsih[1*], Ari Handono Ramelan[2] and Yosep Rio Kristiawan[1]

[1]Inorganic Material Research Group, Faculty of Mathematic and Natural Sciences, Universitas Sebelas Maret, Surakarta, Indonesia
[2]Electronic Materials and Energy Research Group, Faculty of Mathematic and Natural Sciences, Universitas Sebelas Maret, Surakarta, Indonesia

[*]Corresponding author: sayekti@mipa.uns.ac.id

Published online: 30 April 2019
To cite this article: Sayekti Wahyuningsih, Ari Handono Ramelan and Yosep Rio Kristiawan (2019). Transformation of magnetite (Fe_3O_4) and maghemite (γ–Fe_2O_3) to α–Fe_2O_3 from magnetic phase of Glagah iron sand. *Journal of Engineering Science*, 15, 11–21, https://doi.org/10.21315/jes2019.15.2.
To link to this article: https://doi.org/10.21315/jes2019.15.2

Abstract: *The study of magnetite (Fe_3O_4) and maghemite (γ-Fe_2O_3) transformation to α-Fe_2O_3 from magnetic phase of Glagah iron sand has been done. Glagah sand was magnetised to separate magnetic and non-magnetic sand. Then, it was prepared by ball milling for 5 h (20:1 w/w) to reduce the particle size. Magnetic iron sand was roasted at 1,000°C with the addition of sodium carbonate (Na_2CO_3) (sand mass ratio: Na_2CO_3 1:2 w/w) for 2 h to reduce the silicon dioxide (SiO_2) content. Characterisation of X-ray fluorescence after magnetic separation, ball milling and roasting showed an increasing percentage of Fe_2O_3 from 31.10% to 70.13%. Furthermore, magnetic iron sand was refluxed using hydrochloric acid (HCl) with concentrations of 3, 6, 9 and 12 M for 2 h. Then, the aqueous phase was precipitated with the addition of 3 M ammonium hydroxide (NH_4OH). The obtainable sediments showed Fe_2O_3 optimal percentage at concentration of 12 M by 67.96%. Calcination of Fe_2O_3 at 400°C, 600°C and 800°C showed a phase transformation of Fe_3O_4 and γ-Fe_2O_3 to α-Fe_2O_3 which reached an optimum was 92.23% at a temperature calcination of 800°C was showed an optimum percentage (92.23%) of phase transformation of Fe_3O_4 and γ-Fe_2O_3 to α-Fe_2O_3 at a temperature of 800°C. While the thermogravimetry/different thermal analysis showed the formation of a stable α-Fe_2O_3 after a temperature at 707.9°C is indicated by no longer mass loss.*

Keywords: magnetite, maghemite, iron sand, Glagah, magnetic phase

1. INTRODUCTION

Indonesia was the biggest archipelago country in the world with abundance of natural resources, which one was iron sand. The iron sand is spread almost through all islands in Indonesia with diverse percentage. According to previous studies, Aceh iron sand has a 92% (Fe) contents.[1,2] Sulawesi, Maluku and Jayapura has around 70.07% Fe contents whereas Lumajang, Sukabumi and Glagah have 85%, 50.48% and 48.08% respectively. Iron sand contained major element that already applied in several industrial sector (α-Fe_2O_3) such as pig iron for steel, flexible lithium ion batteries (FLIB), red pigment for paint and high performance supercapacitor electrode.[3,4,5,6]

Iron sand has magnetic compounds Fe(II) and Fe(III) oxide such as, magnetite (Fe_3O_4), ilmenite ($FeTiO_3$), hematite (Fe_2O_3) and other minerals (non-magnetic compounds) like alumina, silica, vanadium and titanium oxide.[7] Predominant compounds of Fe_3O_4 and Fe_2O_3 could be extracted by magnetic separation, such as pyrometallurgy and hydrometallurgical methods. Magnetite (Fe_3O_4) is easily separated through the magnet from iron sand because of their high magnetic characteristic. However, their thermal stability was unstable in high temperature (> 500°C) for electronic applications while hematite (Fe_2O_3) has higher benefits for it electronic applications.[8] Hematite has several polymorph phases, such as alpha, beta, gamma and epsilon. Beta phase (β-Fe_2O_3) has cubic-face-centered and epsilon phase (ε-Fe_2O_3) has orthorombic structure, which both of phases were metastable transition phases. Maghemite (γ-Fe_2O_3) was Fe(III) oxide that has cubic-spinel structure which stable below 300°C and transformed to α-Fe_2O_3 (> 500°C) clearly.[8,9]

The reddish-brown colour alpha hematite (α-Fe_2O_3) was the most stable phase of hematite which has high thermal stability. The α-Fe_2O_3 has been use for electronic applications.[10] Meanwhile, the used of Glagah iron sand could enrich the natural resources of magnetic phase material to form α-Fe_2O_3 beside used the precursors.

In this study have been transformed the Fe_3O_4 and γ-Fe_2O_3 to α-Fe_2O_3 from magnetic phase of Glagah iron sand by magnetic separation, pyrometallurgy and hydrometallurgical methods. In this study, the Fe_3O_4 and γ-Fe_2O_3 from Glagah iron sand magnetic phases has been transformed to α-Fe_2O_3 by magnetic separation, pyrometallurgy and hydrometallurgical methods.

2. EXPERIMENTAL METHOD

2.1 Preparation of Glagah Iron Sand

Glagah iron sand was inducted by magnet to separate the magnetic and non-magnetic phase. The separation of Glagah iron sand repeated by 10 times continuously. Mechanical ball-milling process was done to decrease particle size of magnetic phase (20:1 w/w) in 5 h. Then, the obtainable inducted iron sand was then inducted 10 times continuously again to increase purity of magnetic phase.

2.2 Pyrometallurgical Method

Glagah iron sand was roasted at 1,000°C (2 h) with addition of sodium carbonate (Na_2CO_3) (1:2 w/w). Further, it was dissolved at 90°C distilled water in 2 h and filtered. The iron oxide sediment was analysed using X-ray fluorescence (XRF), X-ray diffraction (XRD) and scanning electron microscope (SEM).

2.3 Hydrometallurgical Method

The sediment dissolved in hydrochloric acid (HCl) 37% at various concentrations 3, 6, 9, 12 M. The iron oxide sediment refluxed at 90°C for 2 h. Furthermore, the solution was filtered to separate sediment and filtrate.

2.4 Transformation of α-Fe_2O_3 from Fe_3O_4 and γ-Fe_2O_3

Ammonium hydroxide (NH_4OH) 3 M was added in leached filtrate until neutral pH 7. The neutralised solution was filtered to obtain filtrate and sediments. The sediments were dried and characterised using XRF to determine the optimum percentage of Fe_2O_3. The optimum Fe_2O_3 were treated at various calcinations temperature, 400°C, 600°C and 800°C. Transformations phase from Fe_3O_4 and γ-Fe_2O_3 to α-Fe_2O_3 were observed using XRD, SEM and thermal gravimetry/different thermal analysis (TG/DTA).

3. RESULTS AND DISCUSSIONS

Physically, Glagah iron sand seemed like black coarse grain with slightly shiny glass sparkle under the lights. Identification of Glagah iron sand contents using XRF can be seen in Table 1. The result of XRF showed that Glagah iron sand has highest compound as silicon dioxide (SiO_2) with 33.48% which followed

by Fe_2O_3 with 31.10%, small amount of calcium oxide (CaO), aluminium oxide (Al_2O_3), titanium dioxide (TiO_2) and traces amount of other content.

Table 1: XRF analysis of Glagah iron sand.

Formula	Compounds (%)	Formula	Compounds (%)
Fe_2O_3	31.10	SrO	0.19
SiO_2	33.48	V_2O_5	0.18
CaO	16.38	Nd_2O_3	0.15
Al_2O_3	7.91	SnO_2	0.07
TiO_2	2.69	ZnO	0.05
K_2O	2.10	Cr_2O_3	0.03
Cl	1.70	ZrO_2	0.03
P_2O_5	1.65	Y_2O_3	0.02
SO_3	1.38	Ga_2O_3	0.01
MnO	0.84		

Note: K_2O: Kalium oxide; Cl: Chlorine; P_2O_5: Phosphorus pentoxide; SO_3: Sulphur trioxide; MnO: Manganese(II) oxide; SrO: Strontium oxide; V_2O_5: Vanadium pentoxide; Nd_2O_3: Neodymium oxide; SnO_2: Stannic oxide; ZnO: Zinc oxide; Cr_2O_3: Chromium(III) oxide; ZrO_2: Zirconium dioxide; Y_2O_3: Yttrium(III) oxide; Ga_2O_3: Gallium oxide.

Figure 1: The magnetic separation process of Glagah iron sand.

According to pyrometallurgical method, the iron sand magnetic phase has been roasted at 1,000°C for 2 h with Na_2CO_3. The roasted iron sand represented a physical change to a greenish black rock. Physical changes can occur due to chemical reactions in the pyrometallurgical process, where SiO_2 reacted with Na_2CO_3 to produce Na_2O. x SiO_2 (s) that has slightly white colour in the surface.

$$Na_2CO_{3(s)} + xSiO_{2(s)} \rightarrow Na_2O.xSiO_{2(s)} + CO_{2(g)} \quad (1)$$

Sodium carbonate and iron sand will dissociate to produce sodium silicate by releasing carbon dioxide. While the green discolouration is was influenced by ferum oxide hydrate derived from the oxidation process of Fe(II) cation in the forming reaction (FeO) at low temperature which caused the green colour:

$$Fe^{2+} + 2OH^{-} \rightarrow Fe(OH)_2 \rightarrow 2Fe(OH)^{3-} \rightarrow Fe_2O_{3(s)} + 3H_2O_{(l)} \quad (2)$$

$$Fe(OH)_2 \rightarrow FeO_{(s)} + H_2O_{(l)} \quad (3)$$

The stability of ferum(II) oxide is was low at room temperature so when dissolved in water, it could gradually turn into reddish brown due to excessed oxidation of ferum(III) oxide (Fe_2O_3). From roasting process, solids in physical appearance showed at Figure 2 were obtained.

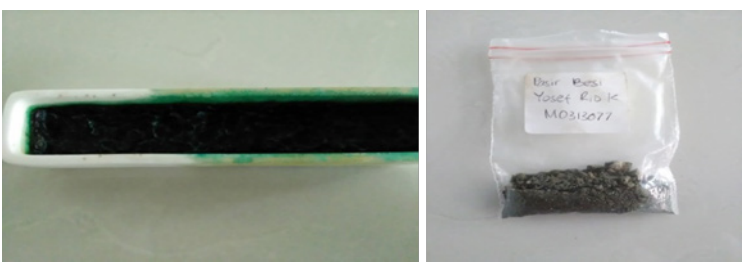

Figure 2: The result of roasting Glagah iron sand with Na_2CO_3.

Magnetic separation, ball milling process and roasting with Na_2CO_3 could effectively increase Fe_2O_3 percentage from 31.10% to 70.13% and decreased SiO_2 content from 33.48% to 11.30%. The XRF analysis shown in Table 2.

Table 2: XRF analysis of magnetic separation and roasting result.

Formula	Compounds (%)	Formula	Compounds (%)
Fe_2O_3	70.13	Pr_6O_{11}	0.11
SiO_2	11.30	ZnO	0.08
TiO_2	6.62	ZrO_2	0.07
CaO	5.17	SnO_2	0.04
K_2O	1.45	BaO	0.04
P_2O_5	1.03	NiO	0.02
Cl	0.97	TeO_2	0.02
MnO	0.92	Ga_2O_3	0.02
SO_3	0.91	I	0.02

(*continued on next page*)

Table 2: (*continued*)

Formula	Compounds (%)	Formula	Compounds (%)
Nd_2O_3	0.44	SrO	0.01
V_2O_5	0.44	Y_2O_3	0.01
Cr_2O_3	0.12	CdO	0.01

Note: Pr_6O_{11}: Praseodymium oxide; BaO: Barium oxide; NiO: Nickel oxide; TeO_2: Tellurium dioxide; I: iodine; CdO: Cadmium oxide.

Extraction of Fe_2O_3 using hydrometallurgical method with various concentrations showed different colours in each solution. The colour difference may occur due to different optimum dissolution of Fe_2O_3 from each variation of HCl concentrations.

$$Fe_2O_{3(s)} + 6H^+Cl^-_{(aq)} \rightarrow 2FeCl_{3(aq)} + 3H_2O_{(l)} \quad (4)$$

Various concentrations of HCl in iron sand solution indicated that the higher concentration of HCl made the colour of the solution is turned to red while the lower concentration of HCl emerged solution in the more pale yellow colour.

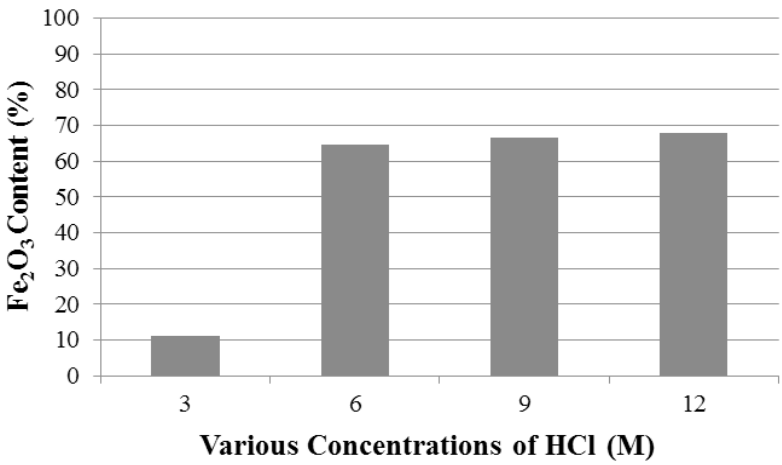

Figure 3: Histogram of Fe_2O_3 in HCl various concentrations.

Leached Fe_2O_3 solution was precipitated by adding NH_4OH 3M continuously until pH 7. The precipitation was occurred by selective reactions at the neutral pH as following reaction:

$$FeCl_3 + 3NH_4OH \rightarrow Fe(OH)_3 + 3NH_4Cl \quad (5)$$

$$2Fe(OH)^{3-} \rightarrow Fe_2O_{3(s)} + 3H_2O_{(l)} \quad (6)$$

The conversion of Fe_3O_4 to Fe_2O_3 may occur as Reaction 5 is controlled by environmental conditions. In this case, the phase change of mixtures of Fe_3O_4 and Fe_2O_3 to be whole Fe_2O_3 could be achieved by increasing the oxidation reaction process at low temperature (90°C). The effective reaction under this condition was a non-redox reaction, which in this reaction was not controlled by the oxidation state but changes in pH. The optimum pH changes could be identified known through the variation of HCl concentration as solvent in the leaching process.

The varied acid conditions in the non-redox reaction could determine the optimum transformation of Fe_3O_4 to Fe_2O_3 which took place at a low temperature (90°C) so that it was possible to obtained phase γ-Fe_2O_3 (< 300°C). The Fe_2O_3 percentage increased significantly at 3 M HCl from 11.06% (3 M HCl) to 64.63% (6 M HCl). Insignificant improvement occurred at concentrations 9 M and 12 M HCl were 66.67% and 67.96% respectively. These results represented that Fe_2O_3 could be optimally dissolved at 12 M HCl to get the highest percentage of α-Fe_2O_3 so the highest percentage of content.

The transformation of Fe_3O_4 and γ-Fe_2O_3 to α-Fe_2O_3 were analysed using XRD. Diffractogram of XRD initial sand (Figure 4[a]) showed that Glagah Sand was natural mineral that has very much noise with no dominant peak. Separation result of Glagah sand (Figure 4[b]) has been formed into some compounds there were TiO_2 rutile (ICSD No. 24277 at $2\theta = 27.63°$) and γ-Fe_2O_3 (ICSD No. 172905 at $2\theta = 35.5°$, 55.73°, 56.98°, 73.89°, 78.28°). The XRD diffractogram analysis shows identified that Fe oxide has been majorly formed in magnetite (Fe_3O_4) and maghemite (γ-Fe_2O_3) phases. Diffractogram of roasted sand (Figure 4[c]) with the addition of Na_2CO_3 at 1000°C. Presented the formation of several compounds with various peaks, there were TiO_2 rutile (ICSD No. 24277 at $2\theta = 27.898°$), Compounds a namely α-Fe_2O_3 (ICSD No. 15840), γ-Fe_2O_3 (ICSD No. 172905), Fe_3O_4 (ICSD No. 49549), TiO_2 rutile (ICSD No. 24277) at $2\theta = 35.862°$, the Compounds B are CaO (ICSD No. 90486), Na_2CO_3 (ICSD No. 1852) at $2\theta = 37.383°$, the Compounds C were α-Fe_2O_3 (ICSD No. 15840), Na_2CO_3 (ICSD No. 1852), MnO (ICSD No. 657304) at $2\theta = 39.352°$, Fe_3O_4 (ICSD No. 49549 at $2\theta = 42.35°$) and TiO_2 rutile (ICSD No. 24277), MnO (ICSD No. 657304) at $2\theta = 68.704°$ that can be seen in Figure 4.

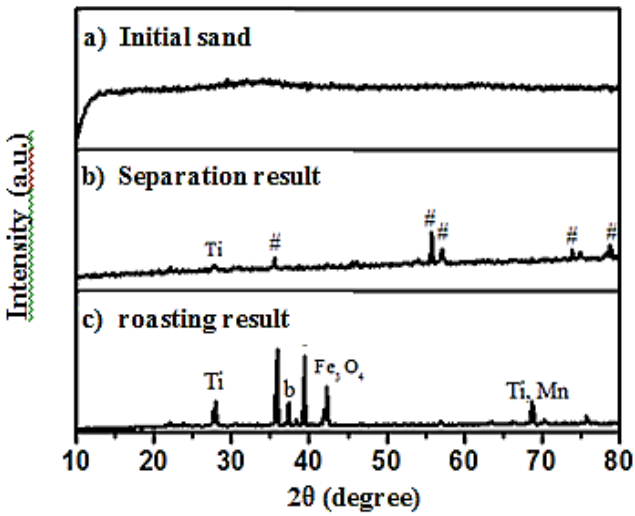

Figure 4: Diffractogram of (a) initial sand, (b) separation result and (c) roasting result.

XRD characterisation after various calcination temperature (400°C, 600°C, 800°C) presented specific diffractogram patterns each other been shown in Figure 5.

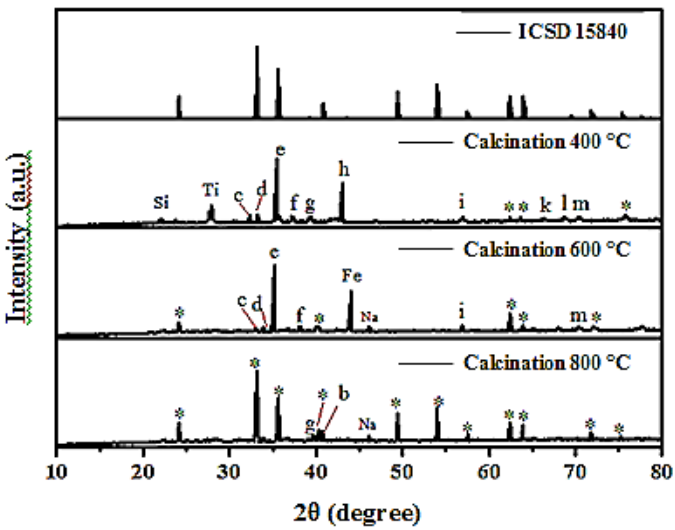

Figure 5: Diffractogram of ICSD 15840, calcination 400°C, calcination 600°C and calcination 800°C.

The diffraction peaks at Figure 5 showed sequential patterns with higher calcination temperature, more visible the transformation of α-Fe_2O_3 phase transformation characterised by the appearance of typical diffraction peaks of α-Fe_2O_3. However, there are still some minor peaks identified as other compounds such as Na_2CO_3, MnO, $NaTiO_2$, Na_2O indicated that there was strong interaction among α-Fe_2O_3 with the compounds. Dominant impurities of Na and Mn were still appeared in the Fe_2O_3 because they acted as cations forming cluster salt (reactionary residue) to prevent instability charge at α-Fe_2O_3. When compared to ICSD 15840, the diffraction peak of Fe_2O_3 at calcination 800°C was the closest match to α-Fe_2O_3. Percentage of α-Fe_2O_3 was calculated by investigating peak intensity ratio α-Fe_2O_3 with peaks of other compounds emerged in the diffractogram and resulted obtained purity of α-Fe_2O_3 was 92.23%.

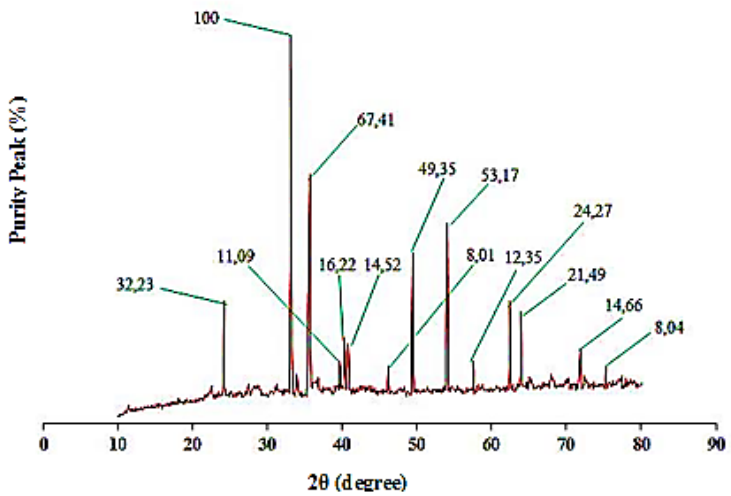

Figure 6: XRD Purity Peak Counts using software Match 3.0.

Related to XRD characterisation result, TG/DTA thermogram was used to confirm thermal stability of α-Fe_2O_3. TG thermogram showed the presence of two stages of mass degradation in the temperature range. The loss of 15.30% mass at first stage in temperature range between 35°C–333.8°C might due to the loss of surface water and organic compounds in α-Fe_2O_3. While DTA thermogram showed that there was an endothermic peak at 79.9°C. The second stage emerged there was a slight mass loss (2.73%) occurring in temperature range between 333.8°C–707.9°C. The mass loss was possible for the phase transition of α-Fe_2O_3 formation although there was relatively no endothermic peak presented in range 333.8°C–707.9°C.

The curve shape tends to be parallel to the x-axis (temperature) after 707.9°C which emphasised that α-Fe_2O_3 phase stability has been established. The high temperature oxidation process (800°C) in γ-Fe_2O_3 transformed to α-Fe_2O_3 could convert the remaining Fe_3O_4 to whole α-Fe_2O_3 according to the following reaction.

$$2Fe_3O_{4(mag)} + O_2 \rightarrow 3Fe_2O_{3(hem)}$$

The total percentage of degraded mass from the α-Fe_2O_3 phase forming process was 18.03%, thus the percentage of mass forming α-Fe_2O_3 was 81.97%. This result showed that transformation of Fe_3O_4 and γ-Fe_2O_3 to α-Fe_2O_3 from magnetic phase of Glagah iron sand was successfully performed.

4. CONCLUSION

The magnetic separation and roasting methods could increase Fe_2O_3 content by 70.13%. The leaching with highest concentration of HCl (12 M) could extract the 67.96% Fe_2O_3 effectively. Transformation of Fe_3O_4 and γ-Fe_2O_3 to α-Fe_2O_3 was confirmed by XRD that optimum presence at calcination 800°C which has 92.23% match peaks. It was supported by TG/DTA thermogram that showed stability form after 707.9°C that indicated by no longer mass loss.

5. REFERENCES

1. Wahyuningsih, S., Ramelan, A. H., Pranata, H. P., Hanif, Q. A., Ismoyo, Y. A. & Ichsan, K. F. (2016). Preparation of Fe_2O_3-TiO_2 composite from Sukabumi iron sand through magnetic separation, pyrometallurgy and hydrometallurgy. *J. Phys. Conf. Ser.*, 776, 012026, https://doi.org/10.1088/1742-6596/776/1/012026.
2. Ramelan, A. H., Wahyuningsih, S., Ismoyo, Y. A., Pranata, H. P. & Munawaroh, H. (2016). Preparation of xerogel SiO_2 from roasted iron sand under various acidic solution. *J. Phys. Conf. Ser.*, 776, 012032, https://doi.org/10.1088/1742-6596/776/1/012032.
3. Chirita, M. & Grozescu, I. (2009). Fe_2O_3 nanoparticles, physical properties and their photochemical and photoelectrochemical applications. *POLITEHNICA*, 54(68), 1–8.

4. Arico, A. S., Bruce, P., Scrosati, B., Tarascon, J. M. & Schalkwijk, W. V. (2005). Nanostructured materials for advanced energy conversion and storage devices. *Nat. Mater.*, 4, 366–377, https://doi.org/10.1038/nmat1368.
5. Balogun, M. S., Wu, Z., Luo, Y., Qiu, W., Fan, X., Long, B., Huang, M., Liu, P. & Tong, Y. (2016). High power density nitridated hematite (α-Fe_2O_3) nanorods as anode for high-performance flexible lithium ion batteries. *J. Power Sources*, 308, 7–17, https://doi.org/10.1016/j.jpowsour.2016.01.043.
6. Shivakumara, S., Penki, T. R. & Munichandraiah, N. (2014). High specific surface area α-Fe_2O_3 nanostructures as high performance electrode material for supercapacitors. *Mater. Lett.*, 131, 100–103, https://doi.org/10.1016/j.matlet.2014.05.160.
7. Baba, A. A., Adekola, F. A., Arodola, O. A., Ibrahim, L., Bale, R. B., Ghosh, M. K. & Sheik, A. R. (2012). Simultaneous recovery of total iron and titanium from ilmenite ore by hydrometallurgical processing. *Metall. Mater. Eng.*, 18(1), 67–78.
8. Darezereshki, E., Bakhtiari, F., Alizadeh, M., Vakylabad, A. B. & Ranjbar, M. (2012). Direct thermal decomposition synthesis and characterization of hematite (α-Fe_2O_3) nanoparticles. *Mater. Sci. Semicond. Process.*, 15(1), 91–97, https://doi.org/10.1016/j.mssp.2011.09.009.
9. Fang, M., Strom, V., Olsson, R. T., Belova, L. & Rao, K. V. (2012). Particle size and magnetic properties depence on growth temperature for rapid mixed co-precipitated magnetite nanoparticle. *Nanotechnol.*, 23, 145601, https://doi.org/10.1088/0957-4484/23/14/145601.
10. Lassoued, A., Lassoued, M. S., Dkhil, B., Ammar, S. & Gadri, A. (2018). Synthesis, structural, morphological, optical and magnetic characterization of iron oxide (α-Fe_2O_3) nanoparticles by precipitation method: Effect of varying the nature of precursor. *Physica E Low Dimens. Syst. Nanostruct.*, 97(4), 328–334, https://doi.org/10.1016/j.physe.2017.12.004.